Polymer Chemistry

RSC Publishing

PAPER

View Article Online
View Journal | View Issue

Cite this: *Polym. Chem.*, 2013, **4**, 1056

Exploring shape amphiphiles beyond giant surfactants: molecular design and click synthesis†

Kan Yue,[a] Chang Liu,[a] Kai Guo,[a] Kan Wu,[a] Xue-Hui Dong,[a] Hao Liu,[a] Mingjun Huang,[a] Chrys Wesdemiotis,[ab] Stephen Z. D. Cheng*[a] and Wen-Bin Zhang*[a]

Received 22nd October 2012
Accepted 1st November 2012

DOI: 10.1039/c2py20881d

www.rsc.org/polymers

This paper reports the molecular design and click syntheses of novel shape amphiphiles with molecular architectures beyond conventional giant surfactants. They include (1) the giant bolaform surfactant which consists of a polystyrene (PS) chain tethered with one hydrophilic POSS cage at each end of the chain (DPOSS–PS–DPOSS); (2) the giant gemini surfactant which contains two hydrophilic POSS cages and two PS tails tethered at one junction point (2DPOSS–2PS); and (3) the multi-headed giant surfactant which is composed of three hydrophilic POSS cages tethered at one end of a PS chain (3DPOSS–PS). The syntheses were achieved in a modular and efficient fashion following the sequential click approach in good yields, providing easy access to a family of shape amphiphiles with precise chemical structures and fine-tuned interactions for a systematic study of structure–property relationships.

Introduction

Shape amphiphiles are composed of building blocks with distinct shapes and are predicted to generate various ordered structures *via* the self-assembly processes driven by both chemical incompatibility and geometric incommensurateness.[1–4] The nano-sized three-dimensional cage structure and readily modifiable peripheral groups make molecular nanoparticles (MNPs), such as functionalized polyhedral oligomeric silsesquioxanes (POSS)[5–9] and [60]fullerene (C_{60}),[10–12] as ideal building blocks for shape amphiphiles.[7,8] These shape- and volume-persistent MNPs can be used to simulate the compact polar head in small-molecule surfactants, but with much larger sizes. Thus, a unique type of shape amphiphiles called "giant surfactants"[13] consisting of a nanoparticle head tethered with a single polymer tail has been developed as a counterpart of the conventional single-tail small-molecule surfactant and has been successfully synthesized by both "grafting-to"[13–15] and "growth-from"[14,16] strategies with precisely defined structures. For example, a giant surfactant consisting of polystyrene (PS) end-capped with carboxylic acid-functionalized POSS (APOSS–PS) has been synthesized by hydrosilylation and thiol–ene functionalization.[13] It was found to self-organize into different micellar morphologies (spheres, cylinders, and vesicles) in selective solvents.[13] Unlike block copolymers,[17,18] the PS tails in the core of these micelles were found to be highly stretched, a feature reminiscent of small-molecule surfactants.[13,19] So, it is intriguing to explore other varieties of shape amphiphiles[20,21] in analogy to their small-molecule surfactant counterparts.

According to architectural features, small-molecule surfactants can be classified as surfactants (composed of one hydrophilic head and one hydrophobic tail), lipids (one hydrophilic head linked with two hydrophobic tails), bolaform surfactants (two hydrophilic heads linked by one tail), gemini surfactants (dimeric surfactants composed of two heads and two tails), and other multi-headed and/or multi-tailed surfactants.[22–26] It has long been known that these different surfactant architectures result in distinct self-assembly behaviors and physical properties. Two factors, namely, the interactions and the molecular packing parameter (also known as the molecular aspect ratio) between the heads and the tails, are thought to dominate the self-assembly in solution.[19,22,23] How does molecular architecture affect the self-assembly behaviors in the POSS-based "giant surfactant" systems? What are the differences between these behaviors and what are the determining factors? To answer these questions, those unattained corresponding model shape amphiphiles, specifically "giant bolaform surfactants", "giant gemini surfactants", and "multi-headed giant surfactants", need to be synthesized, preferably through a modular and efficient approach, for a systematic study.

The sequential "click" approach that we recently reported provides a promising way to do so.[15] Aiming to fulfill the "click" philosophy,[27,28] this approach uses a series of "click" reactions, namely the copper-catalyzed azide–alkyne cycloaddition (CuAAC) reaction[27,29] and the thiol–ene reaction[30–32] to achieve stoichiometric polymer–MNP ligation and high efficiency in

[a]*Department of Polymer Science, College of Polymer Science and Polymer Engineering, The University of Akron, Akron, OH, 44325-3909, USA. E-mail: wz8@uakron.edu; scheng@uakron.edu; Fax: +1 330 972 8626; Tel: +1 330 990 9801/972 6931*

[b]*Department of Chemistry, The University of Akron, Akron, Ohio 44325-3601, USA*

† Electronic supplementary information (ESI) available: The synthetic schemes and NMR data for compounds **1** and **2** are included. The ^{13}C NMR and FT-IR data of the products listed in Table 1 and the MALDI-TOF mass spectrum of VPOSS–PS–VPOSS are also provided. See DOI: 10.1039/c2py20881d

subsequent simultaneous, multi-site functionalization.[13–16,33] The modularity and generality of this approach have been demonstrated in two polymer systems, hydrophobic polystyrene (PS) and hydrophilic poly(ethylene oxide) (PEO). Its versatility and robustness are again tested in the current work by the synthesis of shape amphiphiles with various architectures (Schemes 1–3).

Herein, we report the molecular design and click syntheses of three novel POSS based shape amphiphiles (Fig. 1): (1) the bolaform giant surfactant which consists of a polystyrene (PS) chain tethered with one hydrophilic POSS cage at each end of the chain (DPOSS–PS–DPOSS) (Scheme 1); (2) the gemini giant surfactant which contains two hydrophilic POSS cages and two PS tails tethered at one junction point (2DPOSS–2PS) (Scheme 2); and (3) the multi-headed giant surfactant which is composed of three hydrophilic POSS cages tethered at one end of a PS chain (3DPOSS–PS) (Scheme 3). The syntheses were achieved in a modular and efficient fashion following the sequential click approach in high yields, providing easy access to a family of shape amphiphiles with precise chemical structures and fine-tuned interactions for a systematic investigation of the structure–property relationships.

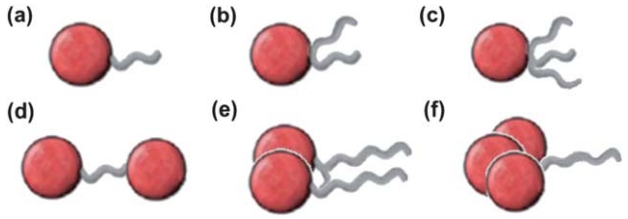

Fig. 1 Schematic illustrations of various types of shape amphiphiles: (a) giant surfactants; (b) giant lipids; (c) multi-tailed giant surfactants; (d) giant bolaform surfactants; (e) giant gemini surfactants; and (f) multi-headed giant surfactants.

Experimental section

Chemicals and solvents

4-Pentynoic acid (98%, Acros Organics), *N*,*N*,*N*′,*N*″,*N*″-pentamethyldiethylenetriamine (PMDETA, 99%, Sigma-Aldrich), 4-dimethylaminopyridine (DMAP, ≥99%, Sigma-Aldrich), *N*,*N*′-diisopropylcarbodiimide (DIPC, 99%, Acros Organics), ethylene glycol (99.8%, Sigma-Aldrich), α-bromoisobutyryl bromide (98%, Sigma-Aldrich), trifluoromethanesulfonic acid (99%, Acros Organics), sodium azide (NaN_3, 99%, Sigma-Aldrich), 2-hydroxy-4′-(2-hydroxyethoxy)-2-methylpropiophenone (Irgacure 2959, 98%, Sigma-Aldrich), 1-thioglycerol (≥98%, Fluka), copper(I) bromide (98%, Acros Organics), 2,2-bis(bromomethyl)-1,3-propanediol (98%, Sigma-Aldrich), pentaerythritoltribromide (98%, TCI America), and OctaVinyl-POSS (OVPOSS, >97%, Hybrid Plastics) were used as received. Toluene (ACS grade, EMD), methanol (reagent grade, Fisher Scientific), chloroform (Certified ACS, Fisher Scientific), dichloromethane (DCM, Fisher Scientific), tetrahydrofuran (THF, Fisher Scientific), ethyl acetate (Fisher Scientific), *N*,*N*-dimethylformamide (DMF, anhydrous 99.8%, Sigma-Aldrich), and hexanes (Certified ACS, Fisher Scientific) were used as received. Silica gel (Sorbent Technologies Inc., 230–400 mesh) was activated by heating to 140 °C for 12 hours. Mono-hydroxyl heptavinyl substituted POSS (VPOSS–OH),[34] VPOSS–alkyne,[15] and azide-end-capped PS (PS–N_3 (ref. 11) and N_3–PS–N_3 (ref. 35 and 36)) were synthesized as reported.

Instrumentation and characterization

The ^1H and ^{13}C NMR spectra of the reported compounds were obtained in $CDCl_3$ (99.8% D, Sigma-Aldrich) or in deuterated THF (THF-d_8, 99.5% D, Sigma-Aldrich) for better solubility using a Varian NMRS 500 spectrometer equipped with an auto-sampling robot at 30 °C. The sample concentration in ^1H NMR

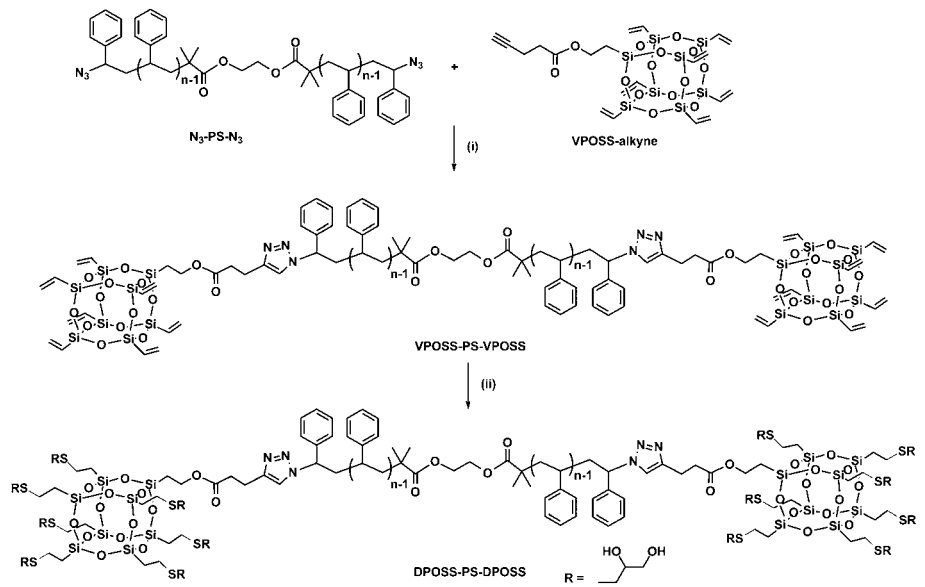

Scheme 1 Synthesis of DPOSS–PS–DPOSS: (i) CuBr, PMDETA, toluene, room temperature, 80%; (ii) 1-thioglycerol, Irgacure 2959, THF, *hν*, 15 min, 78%.

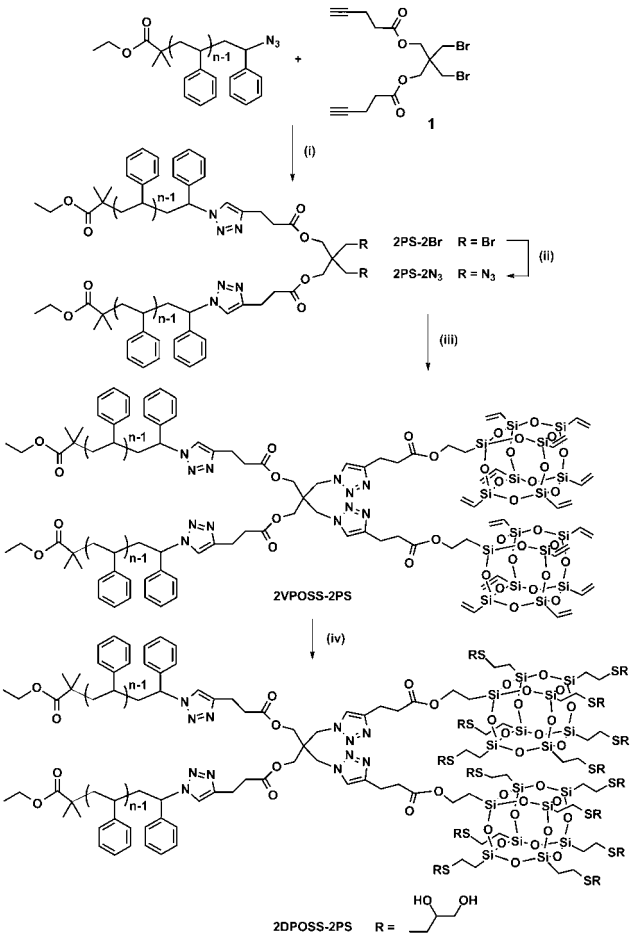

Scheme 2 Synthesis of 2DPOSS–2PS: (i) CuBr, PMDETA, toluene, room temperature, 81%; (ii) NaN_3, DMF, 85 °C, 48 h, 90%; (iii) VPOSS–alkyne (2.1 eq.), CuBr, PMDETA, toluene, room temperature, 80%; (iv) 1-thioglycerol, Irgacure 2959, THF, *hν*, 15 min, 81%.

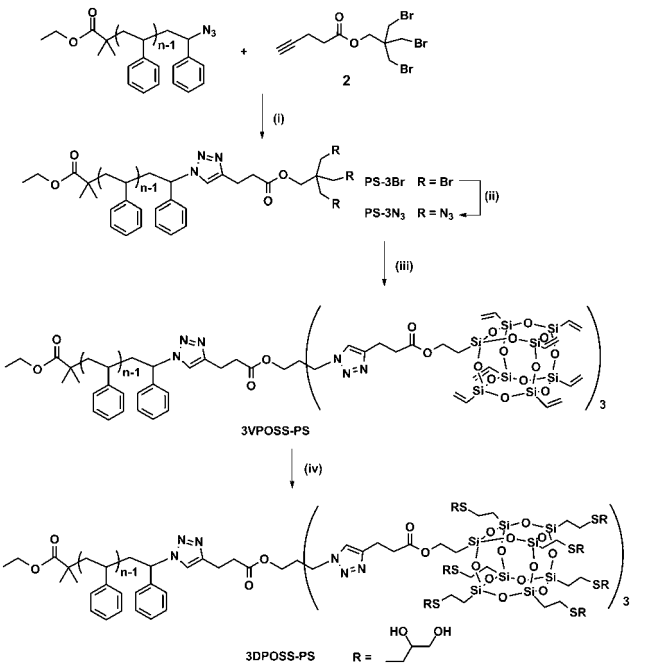

Scheme 3 Synthesis of 3DPOSS–PS: (i) CuBr, PMDETA, toluene, room temperature, 82%; (ii) NaN_3, DMF, 85 °C, 48 h, 91%; (iii) VPOSS–alkyne (3.2 eq.), CuBr, PMDETA, toluene, room temperature, 73%; (iv) 1-thioglycerol, Irgacure 2959, THF, *hν*, 15 min, 75%.

measurements was ~10 to 20 mg mL^{-1}, while it was ~50 to 80 mg mL^{-1} in ^{13}C NMR measurements. The ^1H NMR spectra were referenced to the residual proton impurities in $CDCl_3$ at δ 7.27 ppm (or in THF-d_8 at 3.58 and 1.73 ppm), and ^{13}C NMR spectra were referenced to $^{13}CDCl_3$ at δ 77.00 ppm (or ^{13}C atoms in THF-d_8 at 67.57 and 25.37 ppm). For VPOSS–polymer, the integration ratio between the characteristic vinyl peaks on POSS at δ 6.20–5.85 ppm (21H per VPOSS) and the peaks at δ 7.40–6.35 ppm (aromatic protons in PS) gives the number-average degree of polymerization of the polymer block (DP of PS). The calculated molecular weight ($M_{n,NMR}$) can then be obtained by the summation of $M_{n,polymer}$ (DP × 104.1 g mol^{-1} for PS), $M_{initiator}$, M_{linker}, and M_{XPOSS} (773.2 g mol^{-1} for VPOSS and 1530.3 g mol^{-1} for DPOSS).

Size exclusion chromatograms (SECs) were obtained from a Waters 150-C Plus instrument equipped with three HR-Styragel columns [100 Å, mixed bed (50/500/10^3/10^4 Å), mixed bed (10^3, 10^4, 10^6 Å)], an auto-sampler system and a triple detector system, which included a differential viscometer (Viscotek 100), a differential refractometer (Waters 410), and a laser light scattering detector (Wyatt Technology, DAWN EOS, $\lambda = 670$ nm). The instrument was calibrated with polystyrene standards with molecular weights ranging from ~580 to 841 000 g mol^{-1}. THF was used as the eluent at a flow rate of 1.0 mL min^{-1} at 35 °C. The sample solution was prepared in THF with a concentration of ~5 to 10 mg mL^{-1} depending on the sample's molecular weight and was filtered through a 0.45 μm Teflon filter before injection. Data processing was accomplished using the work station software equipped with the system. Molecular weights from SEC experiments ($M_{n,SEC}$ and $M_{w,SEC}$) and polydispersity indices (PDIs) were obtained from the light scattering detector.

Infrared spectra of polymer products were recorded on an Excalibur Series FT-IR spectrometer (DIGILAB, Randolph, MA) by drop-casting sample films on a KBr plate from polymer solutions in THF (~10 mg mL^{-1}) with subsequent drying at room temperature by blowing air. The data were processed using the Win-IR software.

Matrix-assisted laser desorption/ionization time-of-flight (MALDI-TOF) mass spectra were recorded on a Bruker Ultraflex III TOF/TOF mass spectrometer (Bruker Daltonics, Billerica, MA) equipped with a Nd:YAG laser which emits at 355 nm. The matrix used was *trans*-2-[3-(4-*tert*-butylphenyl)-2-methyl-2-propenylidene]malononitrile (DCTB, >99%, Aldrich) and was dissolved in $CHCl_3$ at a concentration of 20.0 mg mL^{-1}. Sodium trifluoroacetate (NaTFA) was used as the cationizing agent and was dissolved in a mixed solvent of MeOH–$CHCl_3$ (v/v = 1/3) at a concentration of 10.0 mg mL^{-1}. The matrix and cationizing agent solutions were mixed in the ratio of 10/1 (v/v). The sample was prepared by depositing 0.5 μL of the matrix and salt mixture onto the wells of a 384-well ground-steel plate, allowing the spots to dry, depositing 0.5 μL of each sample onto a spot of the

dry matrix, and adding another 0.5 μL of the matrix and salt mixture on top of the dry sample (the sandwich method).[37] Mass spectra were measured either in the reflection mode or in the linear mode, and the mass scale was calibrated externally with a PMMA or PS standard at the molecular weight region under consideration. Data analyses were conducted with the Bruker's flexAnalysis software.

Electrospray ionization mass spectrometry (ESI-MS) experiments were performed with a Waters Synapt HDMS quadrupole/time-of-flight (Q/ToF) mass spectrometer (Waters, Milford, MA). The sprayed solutions were prepared by dissolving 0.5 mg of sample in 1.0 mL of MeOH–$CHCl_3$ solvent mixture (v/v, 50/50). Sodium trifluoroacetate (NaTFA) was used as the cationizing agent and was dissolved in a mixed solvent of MeOH–$CHCl_3$ (v/v = 1/3) at a concentration of 10.0 mg mL^{-1}. Data analysis was conducted using the MassLynx 4.1 and DriftScope 2.1 programs of Waters.

Synthesis of compound **1.** The structure of compound **1** is shown in Scheme 2 and the reaction is shown in Scheme S1 in the ESI.† To a 50 mL round-bottomed flask equipped with a magnetic stirring bar were added 2,2-bis(bromomethyl)-1,3-propanediol (400 mg, 1.53 mmol), 4-pentynoic acid (330 mg, 3.37 mmol) and DMAP (38 mg, 0.3 mmol), followed by the addition of 10 mL of freshly dried CH_2Cl_2 to fully dissolve all the solids. The mixture was capped by a rubber septum, cooled to 0 °C and stirred at that temperature for 10 min, and then DIPC (505 mg, 627 μL, 4.00 mmol) was added dropwise *via* a syringe. The mixture was allowed to room temperature and further stirred for 24 h to complete the reaction. After that, the mixture was filtered and the filtrate was washed with water and brine, dried over Na_2SO_4 and evaporated under vacuum. The residue was purified by flash column chromatography (silica gel, with hexanes–CH_2Cl_2 = 2/1 as the eluent) to afford the product as a clear oil (568 mg). Yield: 88%. ^{1}H NMR ($CDCl_3$, 500 MHz, ppm): δ 4.23 (s, 4H), 3.54 (s, 4H), 2.60 (m, 4H), 2.52 (m, 4H), 2.01 (m, 2H) (shown in Fig. S1a in the ESI†). ^{13}C NMR ($CDCl_3$, 125 MHz, ppm): δ 170.8, 82.1, 69.4, 63.4, 42.5, 33.4, 33.3, 14.4 (shown in Fig. S1b†). MS (ESI, *m*/*z*): calcd mono-isotopic mass for $[M\cdot Na]^+$ ($C_{15}H_{18}Br_2NaO_4$): 442.9 Da, found 442.5 Da.

Synthesis of compound **2.** The structure of compound **2** is shown in Scheme 3 and the reaction is shown in Scheme S2.† Compound **2** was synthesized similarly to compound **1**. Pentaerythritoltribromide (400 mg, 1.23 mmol), 4-pentynoic acid (145 mg, 1.48 mmol), DMAP (25 mg, 0.20 mmol), and DIPC (227 mg, 282 μL, 1.80 mmol) were used. The crude product was purified by flash column chromatography (silica gel, with hexanes–CH_2Cl_2 = 2/1 as the eluent) to afford the product as a clear oil (448 mg). Yield: 90%. ^{1}H NMR ($CDCl_3$, 500 MHz, ppm): δ 4.25 (s, 2H), 3.56 (s, 6H), 2.61 (m, 2H), 2.53 (m, 2H), 2.02 (m, 1H) (shown in Fig. S2a†). ^{13}C NMR ($CDCl_3$, 125 MHz, ppm): δ 170.6, 82.1, 69.5, 63.9, 42.8, 34.0, 33.3, 14.5 (shown in Fig. S2b†). MS (ESI, *m*/*z*): calcd mono-isotopic mass for $[M\cdot Na]^+$ ($C_{10}H_{13}Br_3NaO_2$): 424.8 Da, found 424.4 Da.

General procedure for the CuAAC click reaction. To a 100 mL Schlenk flask equipped with a magnetic stirring bar were added the azide-functionalized polymer, the corresponding alkynes, CuBr (0.05 eq. per azide group), and freshly distilled toluene (20 mL). The resulting solution was degassed by three freeze–pump–thaw cycles before addition of PMDETA (1.0 eq. per azide group) *via* a pipette. The mixture was further degassed by one freeze–pump–thaw cycle, and was then stirred at room temperature for 12 hours. The solution was then directly transferred onto a silica gel column. Toluene was first used as the eluent to fully remove the excess unreacted starting materials, then a mixture of toluene and ethyl acetate (v/v = 1/1) was used to wash the product off the column. After removing the solvent, the crude product was precipitated into cold MeOH and collected by vacuum filtration once and dried under vacuum to afford the product.

General procedure for the thiol–ene click reaction. To an open vial without a stirring bar were added VPOSS–polymer, 1-thioglycerol (10.0 eq. per VPOSS, or 1.4 eq. per vinyl group), photo-initiator Irgacure 2959 (0.10 eq. per VPOSS, or 0.014 eq. per vinyl group), and a minimum amount of THF to fully dissolve the solids. The reaction completed after irradiation by 365 nm UV light for 15 min. The mixture was then purified by repeated precipitation from concentrated THF solutions of the crude products into cold MeOH–water mixture (v/v = 1/1 to 1/5) and collected by centrifugation.

General procedure for the azide substitution reaction. To a 50 mL round-bottomed flask equipped with a magnetic stirring bar were added the bromo-bearing polymer, sodium azide (10 eq. per bromo group), and anhydrous DMF (4 mL). The mixture was heated to 85 °C and stirred for 48 h before cooling down to room temperature. The mixture was diluted with 10 mL of dichloromethane, washed with water (20 mL) and brine (20 mL), dried over Na_2SO_4, concentrated and precipitated into cold MeOH to afford the azide functionalized polymers.

VPOSS–PS–VPOSS. Following the general procedure for the CuAAC click reaction, N_3–PS–N_3 (M_n = 2.7 kg mol^{-1}, PDI = 1.04, 200 mg, 0.074 mmol), VPOSS–alkyne (115 mg, 0.156 mmol, 2.1 eq.), CuBr (1 mg, 0.007 mmol, 0.1 eq.), and PMDETA (26 mg, 32 μL, 0.15 mmol, 2.0 eq.) were used. VPOSS–PS–VPOSS was obtained as a white powder (278 mg). Yield: 80%. ^{1}H NMR ($CDCl_3$, 500 MHz, ppm): δ 7.40–6.35 (m, 120H), 6.20–5.85 (m, 42H), 5.05 (m, 2H), 4.20 (m, 4H), 3.30 (m, 4H), 2.90 (m, 4H), 2.59 (m, 4H), 2.40–1.20 (m, 72H), 1.15 (m, 4H), 0.96–0.75 (m, 12H). ^{13}C NMR ($CDCl_3$, 125 MHz, ppm): δ 176.8, 172.6, 146.0–144.8, 137.1, 137.0, 129.0–125.4, 120.2, 61.4, 60.7, 48.3, 46.4–39.7, 33.8, 33.7, 30.3, 27.2, 26.8–24.9, 20.9, 13.1 (shown in Fig. S3a in the ESI†). FT-IR (KBr) ν (cm^{-1}): 3062, 3027, 2957, 2926, 2855, 1946, 1734, 1602, 1493, 1450, 1409, 1275, 1119 (Si–O–Si asymmetric stretching), 1008, 971, 910, 766, 700 (shown in Fig. S4b†). MS (MALDI-TOF, *m*/*z*): calcd mono-isotopic mass for $[22mer\cdot Na]^+$ ($C_{228}H_{252}N_6NaO_{32}Si_{16}$): 4056.4 Da, found: 4056.9 Da (shown in Fig. S5†). $M_{n,NMR}$ = 4.2 kg mol^{-1}. SEC: $M_{n,SEC}$ = 3.7 kg mol^{-1}, $M_{w,SEC}$ = 3.8 kg mol^{-1}, PDI = 1.03.

DPOSS–PS–DPOSS. Following the general procedure for the thiol–ene click reaction, VPOSS–PS–VPOSS (M_n = 4.2 kg mol^{-1}, PDI = 1.03, 100 mg, 0.024 mmol), 1-thioglycerol (52 mg, 0.48 mmol, 20 eq.), Irgacure 2959 (1 mg, 0.0048 mmol, 0.2 eq.), and 2 mL of THF were used. DPOSS–PS–DPOSS was collected as a white powder (105 mg). Yield: 78%. ^{1}H NMR (THF-d_8, 500 MHz, ppm): δ 7.40–6.35 (m, 120H), 5.10 (m, 2H), 4.50–3.80

(m, 32H), 3.80–3.20 (m, 46H), 3.20–2.40 (m, 64H), 2.30–1.20 (m, 72H), 1.25–0.60 (m, 44H). ^{13}C NMR (THF-d_8, 125 MHz, ppm): δ 176.9, 173.1, 146.8–145.8, 129.6–126.0, 73.0, 66.3, 62.5, 61.2, 46.0–41.0, 36.3, 34.5, 30.9, 27.5, 21.9, 14.1 (Fig. S3b in the ESI†). FT-IR (KBr) ν (cm^{-1}): 3386, 3061, 3027, 2924, 2870, 1952, 1881, 1804, 1602, 1492, 1451, 1283, 1123 (Si–O–Si asymmetric stretching), 1031, 909, 760, 701 (shown in Fig. S4c†). $M_{n,NMR}$ = 5.6 kg mol^{-1}. SEC: $M_{n,SEC}$ = 5.6 kg mol^{-1}, $M_{w,SEC}$ = 6.0 kg mol^{-1}, PDI = 1.07.

2PS–2Br. Following the general procedure for the CuAAC click reaction, compound **1** (40 mg, 0.095 mmol), PS–N_3 (M_n = 2.0 kg mol^{-1}, PDI = 1.09, 400 mg, 0.20 mmol, 2.1 eq.), CuBr (1.5 mg, 0.01 mmol, 0.1 eq.), and PMDETA (35 mg, 42 μL, 0.2 mmol, 2.0 eq.) were used. 2PS–2Br was obtained as a white powder (341 mg). Yield: 81%. ^{1}H NMR ($CDCl_3$, 500 MHz, ppm): δ 7.40–6.35 (m, 180H), 5.06 (m, 2H), 4.11 (m, 4H), 3.60 (m, 4H), 3.38 (m, 4H), 2.94 (m, 4H), 2.69 (m, 4H), 2.60–1.20 (m, 108H), 1.10–0.90 (m, 18H). ^{13}C NMR ($CDCl_3$, 125 MHz, ppm): δ 177.4, 171.7, 146.0–145.0, 128.8–125.3, 120.1, 63.0, 59.9, 48.4, 46.4–40.0, 33.4, 33.3, 26.9–24.9, 20.8, 13.9 (shown in Fig. S6a in the ESI†). FT-IR (KBr) ν (cm^{-1}): 3083, 3061, 3027, 2927, 2854, 1945, 1873, 1804, 1745, 1727, 1602, 1552, 1494, 1453, 1387, 1364, 1068, 1029, 909, 862, 759, 699 (shown in Fig. S7b†). MS (MALDI-TOF, *m*/*z*): calcd mono-isotopic mass for [30mer·Na]$^+$ ($C_{267}H_{280}Br_2N_6NaO_8$): 3879.0 Da, found: 3879.4 Da. $M_{n,NMR}$ = 4.5 kg mol^{-1}. SEC: $M_{n,SEC}$ = 4.7 kg mol^{-1}, $M_{w,SEC}$ = 4.8 kg mol^{-1}, PDI = 1.02.

2PS–2N$_3$. Following the general procedure for the azide substitution reaction, 2PS–2Br (M_n = 4.5 kg mol^{-1}, PDI = 1.02, 200 mg, 0.044 mmol) and sodium azide (29 mg, 0.44 mmol, 10 eq.) were used. 2PS–$2N_3$ was obtained as a white powder (177 mg). Yield: 90%. ^{1}H NMR ($CDCl_3$, 500 MHz, ppm): δ 7.40–6.35 (m, 180H), 5.07 (m, 2H), 3.96 (m, 4H), 3.60 (m, 4H), 3.28 (m, 4H), 2.93 (m, 4H), 2.71 (m, 4H), 2.60–1.20 (m, 108H), 1.10–0.90 (m, 18H). ^{13}C NMR ($CDCl_3$, 125 MHz, ppm): δ 177.4, 171.9, 146.0–144.8, 128.8–125.3, 120.0, 63.1, 62.4, 59.9, 51.1, 48.5, 46.5–39.8, 33.3, 29.7, 26.9–24.9, 20.8, 13.9 (shown in Fig. S6b in the ESI†). FT-IR (KBr) ν (cm^{-1}): 3083, 3061, 3027, 2926, 2854, 2104 (the azide group), 1947, 1875, 1805, 1747, 1726, 1680, 1602, 1550, 1493, 1453, 1386, 1365, 1182, 1068, 1029, 908, 759, 699 (shown in Fig. S7c†). MS (MALDI-TOF, *m*/*z*): calcd mono-isotopic mass for [30mer·Na]$^+$ ($C_{267}H_{280}N_{12}NaO_8$): 3805.2 Da, found: 3805.5 Da. $M_{n,NMR}$ = 4.4 kg mol^{-1}. SEC: $M_{n,SEC}$ = 4.3 kg mol^{-1}, $M_{w,SEC}$ = 4.4 kg mol^{-1}, PDI = 1.02.

2VPOSS–2PS. Following the general procedure for the CuAAC click reaction, 2PS–$2N_3$ (M_n = 4.4 kg mol^{-1}, PDI = 1.02, 150 mg, 0.034 mmol), VPOSS–alkyne (52 mg, 0.071 mmol, 2.1 eq.), CuBr (0.5 mg, 0.0034 mmol, 0.1 eq.), and PMDETA (12 mg, 15 μL, 0.068 mmol, 2.0 eq.) were used. 2VPOSS–2PS was obtained as a white powder (160 mg). Yield: 80%. ^{1}H NMR ($CDCl_3$, 500 MHz, ppm): δ 7.67 (m, 2H), 7.40–6.35 (m, 180H), 6.20–5.85 (m, 42H), 5.05 (m, 2H), 4.25 (m, 4H), 4.13 (m, 6H), 3.65 (m, 8H), 3.00 (m, 8H), 2.69 (m, 8H), 2.60–1.20 (m, 110H), 1.10–0.90 (m, 18H). ^{13}C NMR ($CDCl_3$, 125 MHz, ppm): δ 177.4, 172.4, 171.5, 146.0–144.8, 137.1, 137.0, 129.0–125.4, 123.8, 120.1, 61.8, 60.8, 59.9, 48.7, 46.4–40.3, 33.5, 33.1, 30.3, 29.7, 26.8–24.9, 20.8, 13.9, 13.2 (shown in Fig. S6c in the ESI†). FT-IR (KBr) ν (cm^{-1}): 3083, 3061, 3027, 2957, 2926, 2854, 1945, 1874, 1803, 1734, 1602, 1553, 1493, 1453, 1408, 1275, 1120 (Si–O–Si asymmetric stretching), 1069, 1008, 970, 909, 760, 699 (shown in Fig. S7d†). MS (MALDI-TOF, *m*/*z*): calcd mono-isotopic mass for [30mer·Na]$^+$ ($C_{309}H_{340}N_{12}NaO_{36}Si_{16}$): 5265.1 Da, found: 5265.3 Da. $M_{n,NMR}$ = 5.9 kg mol^{-1}. SEC: $M_{n,SEC}$ = 5.2 kg mol^{-1}, $M_{w,SEC}$ = 5.3 kg mol^{-1}, PDI = 1.02.

2DPOSS–2PS. Following the general procedure for the thiol–ene click reaction, 2VPOSS–2PS (M_n = 5.9 kg mol^{-1}, PDI = 1.02, 70 mg, 0.012 mmol), 1-thioglycerol (26 mg, 0.24 mmol, 20 eq.), Irgacure 2959 (0.5 mg, 0.0024 mmol, 0.2 eq.), and 2 mL of THF were used. 2DPOSS–2PS was collected as a white powder (71 mg). Yield: 81%. ^{1}H NMR (THF-d_8, 500 MHz, ppm): δ 7.83 (m, 2H), 7.40–6.35 (m, 180H), 5.15 (m, 2H), 4.40–3.75 (m, 38H), 3.75–3.20 (m, 50H), 3.10–2.40 (m, 72H), 2.30–1.20 (m, 110H), 1.25–0.60 (m, 46H). ^{13}C NMR (THF-d_8, 125 MHz, ppm): δ 172.4, 146.0–144.8, 129.0–125.4, 73.0, 66.3, 60.5, 50.1, 46.4–40.3, 36.3, 30.9, 27.6, 23.7, 21.9, 14.6, 14.1 (shown in Fig. S6d in the ESI†). FT-IR (KBr) ν (cm^{-1}): 3389, 3061, 3026, 2924, 1729, 1602, 1493, 1452, 1283, 1181, 1119 (Si–O–Si asymmetric stretching), 1029, 908, 758, 699 (shown in Fig. S7e†). $M_{n,NMR}$ = 7.4 kg mol^{-1}. SEC: $M_{n,SEC}$ = 7.0 kg mol^{-1}, $M_{w,SEC}$ = 7.3 kg mol^{-1}, PDI = 1.04.

PS–3Br. Following the general procedure for the CuAAC click reaction, PS–N_3 (M_n = 4.5 kg mol^{-1}, PDI = 1.03, 300 mg, 0.067 mmol), compound **2** (30 mg, 0.073 mmol, 1.1 eq.), CuBr (0.6 mg, 0.004 mmol, 0.05 eq.), and PMDETA (12 mg, 15 μL, 0.067 mmol, 1.0 eq.) were used. PS–3Br was obtained as a white powder (268 mg). Yield: 82%. ^{1}H NMR ($CDCl_3$, 500 MHz, ppm): δ 7.40–6.35 (m, 205H), 5.10 (m, 1H), 4.21 (m, 2H), 3.60 (m, 2H), 3.49 (m, 6H), 3.00 (m, 2H), 2.77 (m, 2H), 2.60–1.20 (m, 123H), 1.10–0.90 (m, 9H). ^{13}C NMR ($CDCl_3$, 125 MHz, ppm): δ 177.4, 171.6, 146.1–145.0, 128.8–125.3, 120.1, 63.6, 63.5, 63.1, 59.9, 46.4–40.0, 33.9, 33.3, 29.7, 26.9–24.9, 20.9, 13.9 (shown in Fig. S8a in the ESI†). FT-IR (KBr) ν (cm^{-1}): 3060, 3026, 2825, 2852, 1944, 1872, 1804, 1750, 1747, 1601, 1492, 1452, 1364, 1069, 1028, 908, 758, 699 (shown in Fig. S9b†). MS (MALDI-TOF, *m*/*z*): calcd mono-isotopic mass for [40mer·Na]$^+$ ($C_{336}H_{344}Br_3N_3NaO_4$): 4744.4 Da, found: 4745.1 Da. $M_{n,NMR}$ = 4.9 kg mol^{-1}. SEC: $M_{n,SEC}$ = 5.5 kg mol^{-1}, $M_{w,SEC}$ = 5.6 kg mol^{-1}, PDI = 1.02.

PS–3N$_3$. Following the general procedure for the azide substitution reaction, PS–3Br (M_n = 4.9 kg mol^{-1}, PDI = 1.02, 250 mg, 0.051 mmol) and sodium azide (33 mg, 0.51 mmol, 10 eq.) were used. PS–$3N_3$ was obtained as a white powder (222 mg). Yield: 91%. ^{1}H NMR ($CDCl_3$, 500 MHz, ppm): δ 7.40–6.35 (m, 205H), 5.10 (m, 1H), 4.02 (m, 2H), 3.60 (m, 2H), 3.32 (m, 6H), 3.00 (m, 2H), 2.77 (m, 2H), 2.60–1.20 (m, 123H), 1.10–0.90 (m, 9H). ^{13}C NMR ($CDCl_3$, 125 MHz, ppm): δ 177.4, 171.9, 146.0–144.8, 128.8–125.3, 120.1, 63.1, 62.8, 62.7, 59.9, 51.3, 46.4–39.8, 33.4, 33.2, 31.9, 29.7, 29.3, 26.8–24.9, 22.8, 22.7, 20.9, 14.1, 13.9 (shown in Fig. S8b in the ESI†). FT-IR (KBr) ν (cm^{-1}): 3061, 3027, 2925, 2851, 2103, 1944, 1872, 1804, 1749, 1746, 1602, 1494, 1452, 1366, 1301, 1181, 1029, 908, 758, 731, 698 (shown in Fig. S9c†). MS (MALDI-TOF, *m*/*z*): calcd average mass for [40mer·Na]$^+$ ($C_{336}H_{344}N_{12}NaO_4$): 4637.4 Da, found: 4639.0 Da. $M_{n,NMR}$ = 4.8 kg mol^{-1}. SEC: $M_{n,SEC}$ = 5.1 kg mol^{-1}, $M_{w,SEC}$ = 5.3 kg mol^{-1}, PDI = 1.03.

3VPOSS–PS. Following the general procedure for the CuAAC click reaction, PS–$3N_3$ (M_n = 4.8 kg mol^{-1}, PDI = 1.03, 200 mg, 0.042 mmol), VPOSS–alkyne (98 mg, 0.133 mmol, 3.2 eq.), CuBr (1 mg, 0.006 mmol, 0.15 eq.), and PMDETA (22 mg, 26 μL, 0.126 mmol, 3.0 eq.) were used. 3VPOSS–PS was obtained as a white powder (213 mg). Yield: 73%. ^{1}H NMR ($CDCl_3$, 500 MHz, ppm): δ 7.89 (m, 3H), 7.40–6.35 (m, 205H), 6.20–5.85 (m, 63H), 5.10 (m, 1H), 4.28 (m, 6H), 4.16 (m, 6H), 3.65 (m, 4H), 3.05 (m, 8H), 2.87 (m, 2H), 2.74 (m, 6H), 2.60–1.20 (m, 129H), 1.10–0.90 (m, 9H). ^{13}C NMR ($CDCl_3$, 125 MHz, ppm): δ 177.4, 172.3, 171.2, 146.0–144.8, 137.1, 137.0, 129.0–125.4, 124.4, 61.6, 60.8, 59.9, 48.8, 46.4–40.3, 34.2, 33.4, 30.4, 29.7, 26.8–24.9, 20.8, 13.9, 13.2 (shown in Fig. S8c in the ESI†). FT-IR (KBr) ν (cm^{-1}): 3083, 3062, 3027, 2958, 2925, 2855, 1944, 1873, 1736, 1602, 1553, 1493, 1453, 1409, 1365, 1275, 1121 (Si–O–Si asymmetric stretching), 1069, 1030, 1008, 971, 909, 862, 760, 700, 679 (shown in Fig. S9d†). MS (MALDI-TOF, *m*/*z*): calcd mono-isotopic mass for [40mer·Na]$^+$ ($C_{399}H_{434}N_{12}NaO_{46}Si_{24}$): 6824.6 Da, found: 6824.9 Da. $M_{n,NMR}$ = 7.0 kg mol^{-1}. SEC: $M_{n,SEC}$ = 7.3 kg mol^{-1}, $M_{w,SEC}$ = 7.5 kg mol^{-1}, PDI = 1.02.

3DPOSS–PS. Following the general procedure for the thiol–ene click reaction, 3VPOSS–PS (M_n = 7.0 kg mol^{-1}, PDI = 1.02, 120 mg, 0.017 mmol), 1-thioglycerol (56 mg, 0.51 mmol, 30 eq.), Irgacure 2959 (1 mg, 0.005 mmol, 0.3 eq.), and 2 mL of THF were used. 3DPOSS–PS was collected as a white powder (119 mg). Yield: 75%. ^{1}H NMR (THF-d_8, 500 MHz, ppm): δ 7.99 (m, 3H), 7.40–6.35 (m, 205H), 5.15 (m, 1H), 4.50–3.75 (m, 54H), 3.70–3.30 (m, 67H), 3.10–2.35 (m, 100H), 2.60–1.20 (m, 129H), 1.10–0.90 (m, 51H). ^{13}C NMR (THF-d_8, 125 MHz, ppm): δ 147.0–144.8, 129.9–125.4, 73.0, 66.3, 61.4, 60.5, 50.9, 46.4–40.3, 36.3, 30.9, 27.6, 23.7, 21.9, 14.5, 14.1 (shown in Fig. S8d†). FT-IR (KBr) ν (cm^{-1}): 3373 (br), 3027, 2924, 1732, 1646, 1493, 1452, 1385, 1283, 1180, 1117 (Si–O–Si asymmetric stretching), 1030, 908, 758, 699 (shown in Fig. S9e†). $M_{n,NMR}$ = 9.3 kg mol^{-1}. SEC: $M_{n,SEC}$ = 10.0 kg mol^{-1}, $M_{w,SEC}$ = 10.5 kg mol^{-1}, PDI = 1.05.

Results and discussion

Giant bolaform surfactant

Studies on small-molecule surfactants have revealed that molecular architecture is an important factor in tuning their properties and self-assembly behaviors.[23] Bolaform surfactants contain two hydrophilic groups at both ends of a hydrocarbon chain. This feature largely influences the solubility and critical micelle concentration (CMC) of Bolaform surfactants, compared to conventional surfactants.[24] Similarly to block copolymers, A–B–A type triblock copolymers containing two terminal hydrophilic A-blocks are known to behave differently in solution self-assembly processes compared to that of the A–B type amphiphilic diblock copolymers, partly due to the more constrained chain conformation of the hydrophobic B-block in the self-assembled supramolecular structures.[38] Therefore, it is of great interest to study the counterpart in POSS-based shape amphiphiles – the giant bolaform surfactant (Fig. 1). Although similar POSS-double-end-capped polymers have been reported,[39,40] they are mostly limited to POSS with pre-installed hydrophobic substituents such as isobutyl groups. It is nontrivial to achieve diverse surface functional groups on POSS in such systems. Nevertheless, the synthesis is quite straightforward using the sequential click approach that we recently developed since the "clickable" XPOSS precursor, VPOSS–alkyne,[15] can essentially react with azide-functionalized polymers of any composition and architecture.

The synthesis starts with the CuAAC reaction between VPOSS–alkyne and a telechelic PS with two chain-end azide groups (N_3–PS–N_3), which can be prepared from the ATRP of styrene initiated by a bifunctional initiator and subsequent substitution reaction with sodium azide as reported in previous literature.[35,36] To ensure complete conversion of the azide groups on polymers for easy purification, a slight excess amount of VPOSS–alkyne (1.05 eq. per azide group) was used. After reacting overnight, the FT-IR spectrum of the crude product showed complete disappearance of the strong characteristic peak of the azide group at ~2100 cm^{-1} (Fig. S4a and b in the ESI†). Purification of the product was performed by flash chromatography on a silica gel column to remove the excess VPOSS–alkyne, followed by precipitation from THF solution into cold methanol.

Results from various instrumental characterizations confirmed the covalent bonding of VPOSS to the polymer chain. In the ^{1}H NMR spectrum, the resonance peaks from the vinyl groups on the POSS cage appear at 6.20–5.85 ppm, and the proton adjacent to the chain-end functional groups of PS shifts from 4.03 ppm in N_3–PS–N_3 to 5.05 ppm in VPOSS–PS–VPOSS (see Fig. 2a and b). One of the vinyl carbons is clearly observed

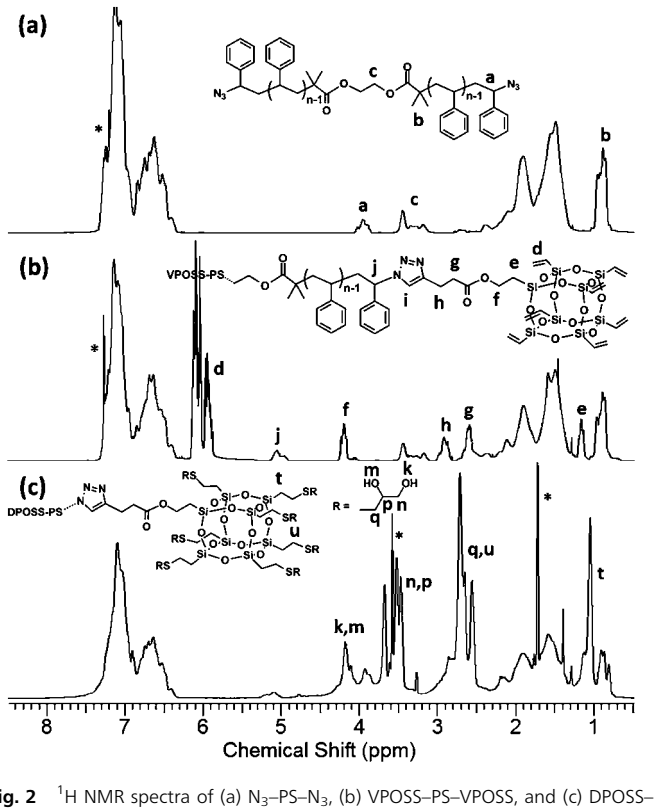

Fig. 2 ^{1}H NMR spectra of (a) N_3–PS–N_3, (b) VPOSS–PS–VPOSS, and (c) DPOSS–PS–DPOSS. The asterisks indicate the peaks from residual protons in the solvents.

in the ^{13}C NMR spectrum at 137.1 ppm (the other one overlaps with the carbons on PS, see Fig. S3a in the ESI†). More convincing evidence comes from the MALDI-TOF MS spectrum. For VPOSS–PS–VPOSS, it exhibits a unimodal symmetric narrow molecular weight distribution with the calculated and observed *m*/*z* matching each other very well (4056.4 Da *versus* 4056.9 Da, see Fig. S5 in the ESI†). The increased molecular weight after the attachment of VPOSS is also reflected by the obvious shift of VPOSS–PS–VPOSS compared with N_3–PS–N_3 in SEC overlay (Fig. 3). From all these evidence, the precisely defined structure of the resulting VPOSS-double-end-capped PS is fully validated.

We have reasoned and demonstrated that the vinyl groups on the POSS periphery can be viewed as a common precursor to varied functional groups such as carboxylic acids, hydroxyl groups, and fluorinated alkyl chains owing to their high reactivity in the thiol–ene click reaction.[15,16,41] As an example, 1-thioglycerol is selected in this study to convert VPOSS to a hydrophilic, fourteen-hydroxyl-functionalized POSS (DPOSS), rendering the hybrid polymer amphiphilicity. Following the general procedure described above, the thiol–ene reaction quantitatively converts the vinyl groups. The structure of the resulting DPOSS–PS–DPOSS is then similarly characterized. As shown in Fig. 2c (also in Fig. S3b†), NMR results confirmed the complete consumption of the vinyl groups by the disappearance of the corresponding peaks. SEC overlay again shows a shift to smaller retention volume due to the increased molecular weight after thiol–ene modification. Although MALDI-TOF mass spectroscopy failed to provide a good spectrum for this sample, probably due to the existence of fourteen sulfur ether linkages after the thiol–ene modification and the relatively high molecular weight, all the other characterization data could guarantee the success of this reaction.

It is worth noting that when the molecular weight of the PS chain is low, the hydrophilic POSS part of the product DPOSS–PS–DPOSS largely increases its solubility in polar solvents such as methanol. Precipitation of the crude product into methanol would give a milky emulsion. Therefore, a mixture of methanol and water was used to facilitate precipitation. A lower molecular weight of the PS chain generally requires a larger volume fraction of water (from 50% to 85% in volume) to maximize mass recovery. In this way, purification of the DPOSS–PS–DPOSS was achieved in a good yield (~80%).

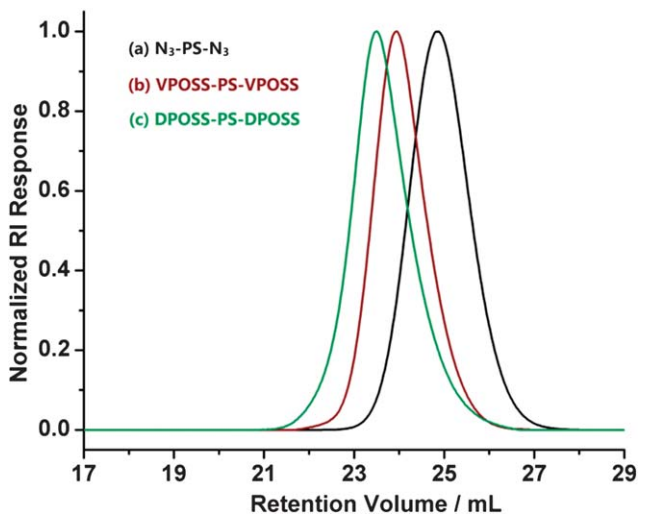

Fig. 3 SEC overlay of (a) N_3–PS–N_3 (black curve), (b) VPOSS–PS–VPOSS (brown curve), and (c) DPOSS–PS–DPOSS (green curve).

Giant gemini surfactant

Besides bolaform surfactants, gemini surfactants represent another common structural variance in specialist surfactants.[25,42,43] In contrast to bolaform surfactants, gemini surfactants are known for their much increased surface activity and decreased aggregation number.[44–46] Small-molecule gemini surfactants may also vary in the length and position of the linker between the two hydrophilic groups, providing another dimension for tuning self-assembly behaviors.[47,48] This inspires us to explore similar dimeric giant surfactants. On the other hand, it is reasoned that two hydrophilic POSS cages located at different positions on a polymer chain might change the intra/inter-molecular interactions between the POSS cages. In this case, a simple model gemini surfactant (2DPOSS–2PS) containing two POSS heads and two PS tails tethered one point with only short linkers is designed (Scheme 2).

The synthetic approach for 2DPOSS–2PS takes advantage of the sequential click strategy by using a "molecular click adaptor" or "molecular click switch" (compound **1** in Scheme 2), which has both "clickable" alkyne groups and latently "clickable" bromo groups. After the first CuAAC reaction between compound **1** and PS–N_3, the bromo groups can be transformed to azide groups, leading to a PS functionalized with two azide groups at the middle of the chain. A second CuAAC click reaction can then be effected to link two VPOSS cages onto the PS chain. All the reactions involved in Scheme 2 are "click-type" reactions, making this post-polymerization modification process extremely efficient and modular. It is anticipated that the method shall be equally applicable to other polymer systems as well.

The molecular click adaptor **1** was synthesized by the Steglich esterification reaction promoted by DIPC and DMAP between 2,2-bis(bromomethyl)-1,3-propanediol and 4-pentynoic acid at room temperature in a very good yield (88%) (see Scheme S1 in the ESI†). The molecular structure and purity of compound **1** is confirmed by ^1H and ^{13}C NMR techniques (Fig. S1†). The ESI MS spectrum also gives an observed *m*/*z* very close to the calculated value (found 442.5 Da *versus* calcd 442.9 Da).

The reaction between compound **1** and PS–N_3 was carried out following the general procedure for the CuAAC reaction. PS–N_3 was added in excess to ensure full consumption of the alkyne groups. The product 2PS–2Br has a larger polarity due to the formation of two triazole linkages, which facilitates the purification by flash column chromatography on silica gel rather than tedious fractionation. Toluene was first used to wash the excess PS–N_3 off the column, and then a mixture of toluene and ethyl acetate (v/v = 1/1) was used to elute the product. Structural characterization of 2PS–2Br was performed by routine techniques. First, 2PS–2Br shows a large shift to smaller retention volume in SEC overlay compared to that of PS–N_3 indicating

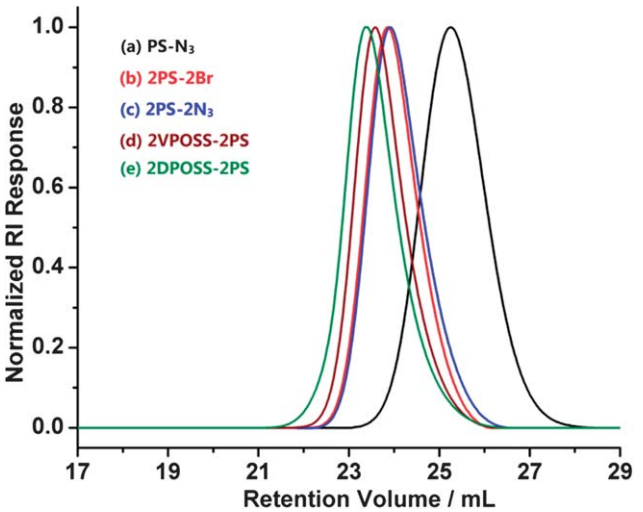

Fig. 4 SEC overlay of (a) PS–N_3 (black curve), (b) 2PS–2Br (red curve), (c) 2PS–$2N_3$ (blue curve), (d) 2VPOSS–2PS (brown curve), and (e) 2DPOSS–2PS (green curve).

dimer formation (see Fig. 4). Moreover, the new peaks appearing in the ^{1}H NMR spectrum can be assigned unambiguously (see Fig. 5a), and the azide peak in the FT-IR spectra fully disappears after this click reaction (see Fig. S7a and b in the ESI†). Last, the MALDI-TOF MS spectrum also gives affirming results of the chemical structure (see Fig. 6a and Table 1).

Conversion of 2PS–2Br to 2PS–$2N_3$ was achieved by reacting with sodium azide at elevated temperature (85 °C).[49] Reaction at room temperature was much slower and usually resulted in incomplete substitution, which could be detected in ^{1}H NMR spectra or the MALDI-TOF MS spectrum by the multiple molecular weight distributions (data not shown). It has been found that a reaction time of 48 hours is enough to completely convert the bromo groups to azide groups. The formation of 2PS–$2N_3$ is clearly supported by the ^{1}H NMR (Fig. 5b) and the MALDI-TOF MS spectra (Fig. 6b). The hydrogens on the bromomethyl groups show resonance peaks at 3.38 ppm, which shift to 3.28 ppm after this reaction. MALDI-TOF MS data again give matched molecular weights and a single molecular weight distribution. In the SEC overlay (Fig. 4), 2PS–$2N_3$ shows a slightly larger retention volume than 2PS–2Br, probably due to the decreased molecular weights after the substitution reaction. In the FT-IR spectrum, the strong peak attributed to the formed azide groups appears at 2104 cm^{-1} (see Fig. S7c in the ESI†).

After the successful synthesis of 2PS–$2N_3$, the proceeding reactions are straightforward following the general synthetic procedures.[15] Again, the intermediate 2VPOSS–2PS and the final product 2DPOSS–2PS were fully characterized by the ^{1}H NMR spectra (see Fig. 5c and d), the ^{13}C NMR spectra (Fig. S6c and d†), the SEC overlay (Fig. 4), and the FT-IR spectra (Fig. S7d and e†). Although the MALDI-TOF mass spectrum of 2VPOSS–2PS shows one single narrow molecular weight distribution and the expected molecular weights, attempts to obtain a mass spectrum of 2DPOSS–2PS with similar quality failed. Again, this is probably due to the high molecular weight and the presence of multiple highly oxidizable sulfur ether linkages which make fragmentation unavoidable and unpredictable.

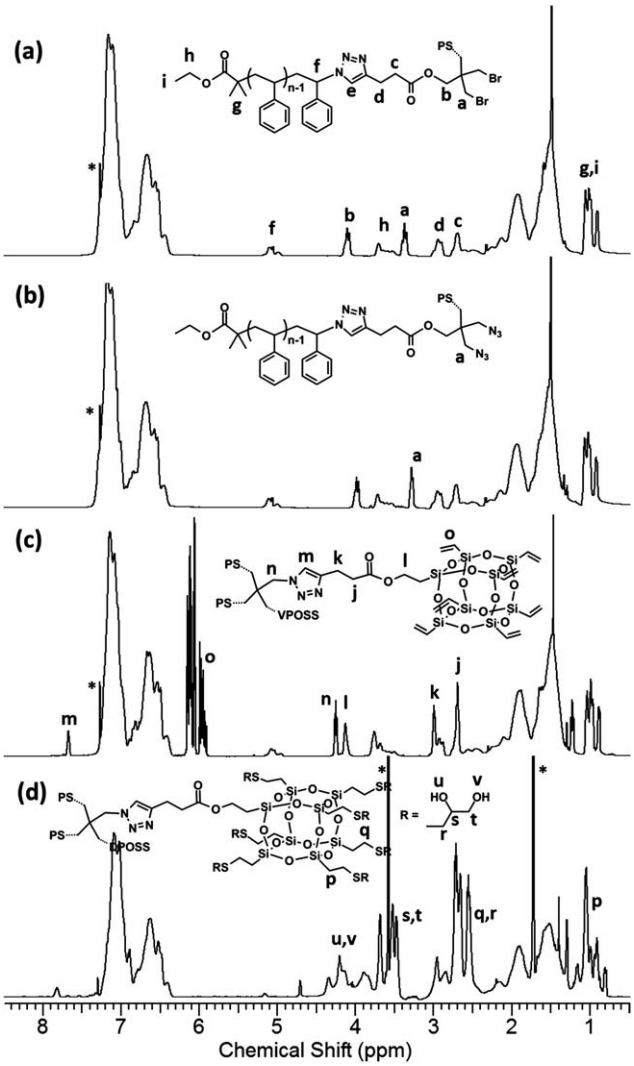

Fig. 5 ^{1}H NMR spectra of (a) 2PS–2Br, (b) 2PS–$2N_3$, (c) 2VPOSS–2PS, and (d) 2DPOSS–2PS. The asterisks indicate the peaks from residual protons in the solvents.

It is also worth mentioning that the hydrogens on the four triazole linkers in 2VPOSS–2PS and 2DPOSS–2PS have two different chemical shifts in the ^{1}H NMR spectra. From Fig. 5a and b, it is clear that hydrogens on the two triazole rings of 2PS–2Br and 2PS–$2N_3$ (proton **e**) cannot be distinguished. We have indirectly proven that they probably overlap with the hydrogens of the PS chain.[15] However, a new peak appears at 7.67 ppm after the second CuAAC click reaction, which can be assigned to proton **m** as shown in Fig. 5c, because integration of this peak tells that it only represents two hydrogens instead of four. This finding is in agreement also with our previous proposal.[15]

Multi-headed giant surfactants

As indicated by our recent report on hydrophilic [60]fullerene based shape amphiphiles, the molecular shape aspect ratio between the hydrophilic part and the hydrophobic part also significantly influences the self-assembly behaviors of shape amphiphiles.[12] For instance, while carboxylic acid

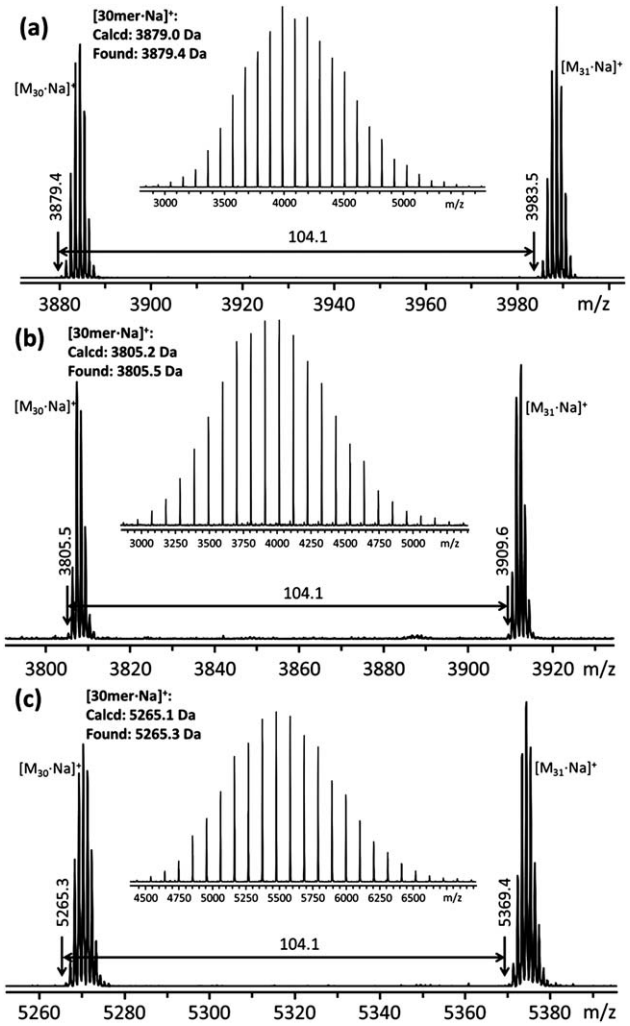

Fig. 6 MALDI-TOF mass spectra of (a) 2PS–2Br, (b) 2PS–2N_3, and (c) 2VPOSS–2PS. All these spectra were obtained in reflection mode with mono-isotopic resolution. The insets show the corresponding full spectra.

functionalized C_{60} (AC_{60}) tethered with one PS tail (PS_n–AC_{60}) forms various micelle structures such as spheres, cylinders and vesicles, AC_{60} tethered with two tails ($2PS_n$–AC_{60}) is found to form only vesicles under identical conditions. This is due to the changed molecular shape aspect ratio of $2PS_n$–AC_{60} that favors the formation of self-assembled structures with less curved interfaces (vesicles).[12] In contrast to these multi-tailed giant surfactants are the multi-headed giant surfactants, whose increased head sizes would favor the inversed packing. It is also intriguing to study the collective effect of a cluster of MNPs on their self-assembly.

The concept of using a "molecular click adaptor/switch" such as compound **1** greatly facilitates the design and synthesis of POSS-based shape amphiphiles of diverse architectures. Another "molecular click adaptor" **2** was designed so as to possess one alkyne group and three bromo groups and was synthesized *via* the Steglich reaction similar to that of **1** (see Scheme 3 and S2 in the ESI†). Following a route similar to that outlined in Scheme 2, a shape amphiphile bearing three hydrophilic DPOSS cages at one end of the chain of a PS tail could be obtained (3DPOSS–PS, see Scheme 3). With three DPOSS cages clustering at one junction point, this molecular design imparts a highly asymmetric ratio at the interface between the hydrophilic part and the hydrophobic part, which is expected to generate intriguing self-assembly behaviors.

The successful synthesis of 3DPOSS–PS again attests to the power of "click" philosophy – building complex molecules from a set of building blocks using a few robust reactions. The reaction sequences are essentially the same in Schemes 2 and 3, but the products, 2DPOSS–2PS and 3DPOSS–PS, have very different molecular architectures. The product of each step has been well characterized and their precisely defined structures are supported by the data from combined routine techniques. In general, the statements and discussions for DPOSS–PS–DPOSS and 2DPOSS–2PS still hold true for the SEC overlay (Fig. 7), the ^{1}H NMR spectra (Fig. 8), the MALDI-TOF MS spectra (Fig. 9), the ^{13}C NMR spectra (Fig. S8†), and the FT-IR spectra (Fig. S9†) of all the intermediate and final products in synthesizing 3DPOSS–PS. One small difference does exist in the SEC overlay (Fig. 7). It is worth noting that after the final thiol–ene click reaction, the retention volume of 3VPOSS–PS and 3DPOSS–PS actually does not change very much whereas for DPOSS–PS–DPOSS and 2DPOSS–2PS, an apparent shift could be

Table 1 Summary of molecular characterization data of the polymer products

Sample	Formula	$M_{n,Calcd}$ (Da)	$M_{n,Found}$ (Da)	$M_{n,NMR}$[d] (kg mol^{-1})	$M_{n,SEC}$[e] (kg mol^{-1})	$M_{w,SEC}$[e] (kg mol^{-1})	PDI[e]
VPOSS–PS–VPOSS	$C_{228}H_{252}N_6NaO_{32}Si_{16}$[a]	4056.4[a]	4056.9[a]	4.2	3.7	3.8	1.03
DPOSS–PS–DPOSS	—	—	—	5.6	5.6	6.0	1.07
2PS–2Br	$C_{267}H_{280}Br_2N_6NaO_8$[b]	3879.0[b]	3879.4[b]	4.5	4.7	4.8	1.02
2PS–2N_3	$C_{267}H_{280}N_{12}NaO_8$[b]	3805.2[b]	3805.5[b]	4.4	4.3	4.4	1.02
2VPOSS–2PS	$C_{309}H_{340}N_{12}NaO_{36}Si_{16}$[b]	5265.1[b]	5265.3[b]	5.9	5.2	5.3	1.02
2DPOSS–2PS	—	—	—	7.4	7.0	7.3	1.04
PS–3Br	$C_{336}H_{344}Br_3N_3NaO_4$[c]	4744.4[c]	4745.1[c]	4.9	5.5	5.6	1.02
PS–3N_3	$C_{336}H_{344}N_{12}NaO_4$[c]	4637.4[c]	4639.0[c]	4.8	5.1	5.3	1.03
3VPOSS–PS	$C_{399}H_{434}N_{12}NaO_{46}Si_{24}$[c]	6824.6[c]	6824.9[c]	7.0	7.3	7.5	1.02
3DPOSS–PS	—	—	—	9.3	10.0	10.5	1.05

[a] These data are based on 22mer with a sodium ion ([22mer·Na]$^+$). [b] These data are based on 30mer with a sodium ion ([30mer·Na]$^+$). [c] These data are based on 40mer with a sodium ion ([40mer·Na]$^+$). [d] These data are calculated based on ^{1}H NMR spectra. [e] These data are obtained from SEC measurements.

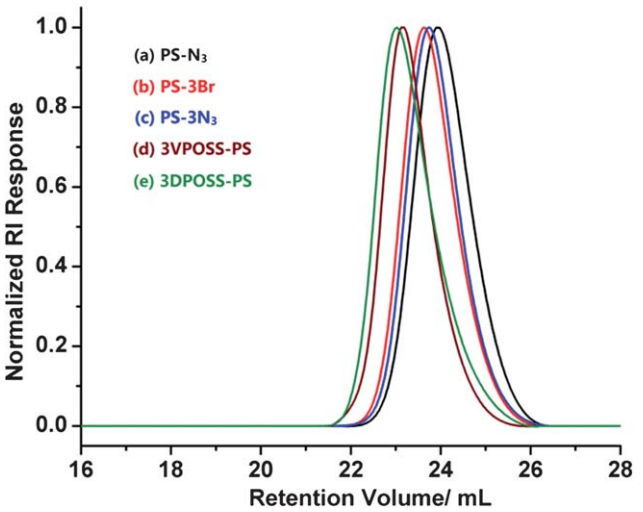

Fig. 7 SEC overlay of (a) PS–N_3 (black curve), (b) PS–3Br (red curve), (c) PS–$3N_3$ (blue curve), (d) 3VPOSS–PS (brown curve), and (e) 3DPOSS–PS (green curve).

clearly seen. This is probably due to the strongest intramolecular interactions of the three DPOSS heads in this case. As a result, the head groups, though bulky, are not as solvated as in the other two cases, thus leading to a smaller hydrodynamic volume than expected.

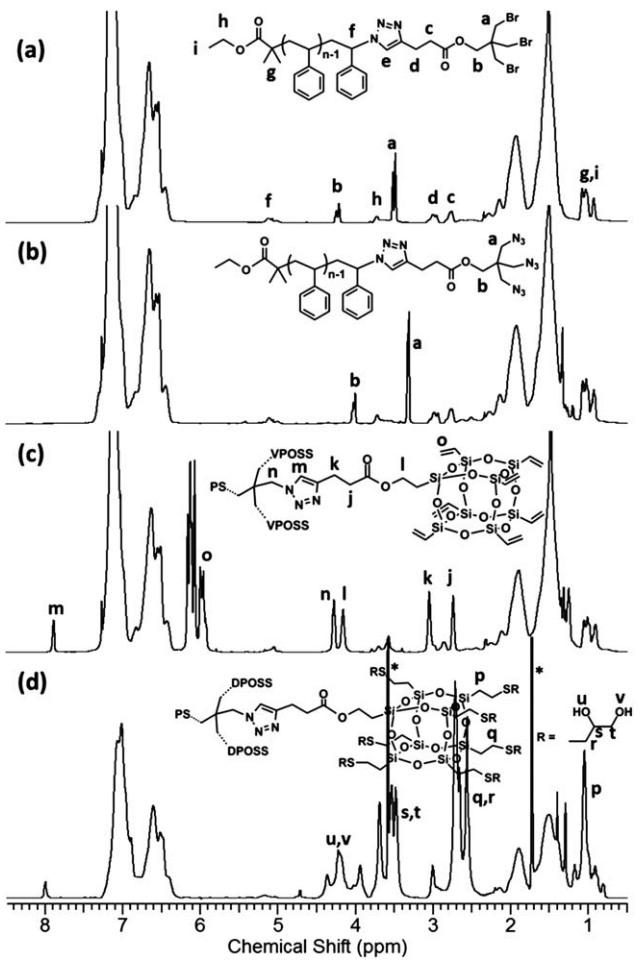

Fig. 8 ^{1}H NMR spectra of (a) PS–3Br, (b) PS–$3N_3$, (c) 3VPOSS–PS, and (d) 3DPOSS–PS. The asterisks indicate the residual protons in the solvents.

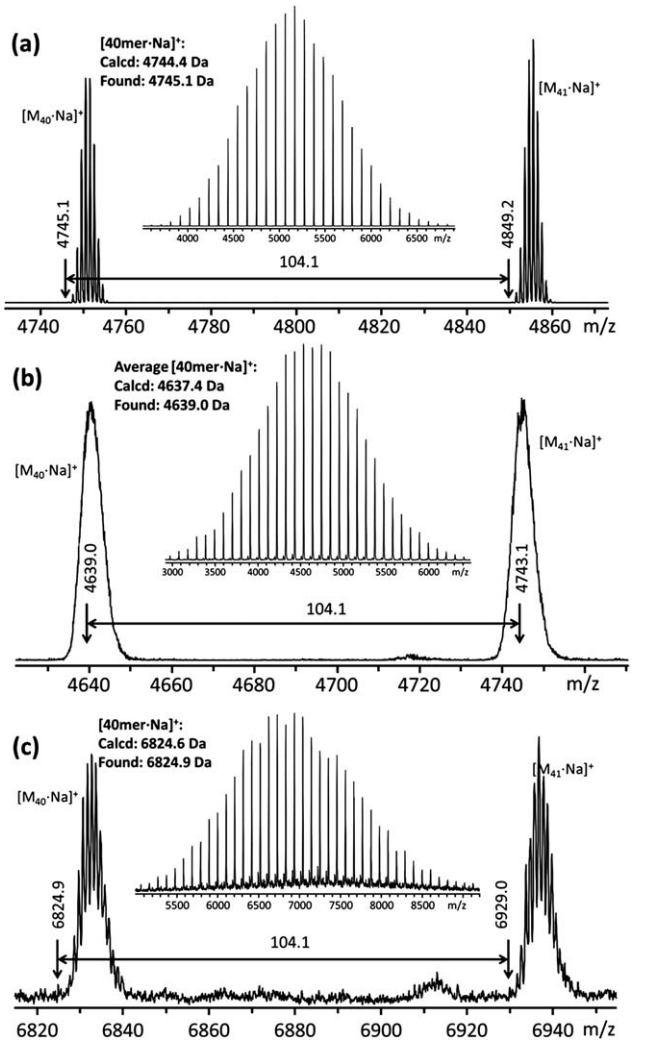

Fig. 9 MALDI-TOF mass spectra of (a) PS–3Br, (b) PS–$3N_3$, and (c) 3VPOSS–PS. Spectra shown in Fig. 5a and c were obtained in reflection mode with isotopic resolution, while the spectrum in Fig. 5b was from the linear mode. The insets show the corresponding full spectra.

Finally, the giant surfactants with multiple hydroxyl-functionalized POSS (DPOSS) cages turn out to be difficult targets for MALDI-TOF mass spectroscopy characterization in general. We were unable to obtain a good MALDI-TOF mass spectrum of 3DPOSS–PS. Nevertheless, the modularity and high efficiency of the thiol–ene click reaction ensure the complete conversion of all the twenty-one vinyl groups in 3VPOSS–PS, which is unambiguously supported by the evidence from SEC and NMR data (see Fig. 7, 8, and S8 in the ESI†). Molecular characterizations of all these new shape amphiphiles are summarized in Table 1. The success of the synthetic approaches shown in Schemes 1–3 further validates that the sequential click strategy is a widely applicable method towards the facile construction of POSS-based shape amphiphiles.[15] This strategy simplifies the molecular design and shall work with materials functionalized with azide groups at any specific positions on the molecule. With the

help of a molecular click adaptor/switch, one can synthesize POSS-polymer based shape amphiphiles with almost any architecture beyond the conventional single-chained giant surfactant.

Conclusion

In summary, three types of novel POSS-based shape amphiphiles have been designed and synthesized with precisely defined structures following the sequential click approach, namely, the giant bolaform surfactant, the giant gemini surfactant, and the multi-headed giant surfactant. By taking advantage of the "molecular click adaptor/switch" molecules as compounds **1** and **2**, the number and position of the nanoparticle head groups are systematically varied to explore the effect of different molecular architectures on the resulted self-assembly behaviors. The modular syntheses can be easily adapted further to other POSS-based shape amphiphiles of even more complex architectures, such as POSS-tethered randomly to one block of a block copolymer, dendrimers with surface decorated with multiple functionalized POSS cages, and even macromolecules or dendrimers based on pure POSS building blocks. The possibility is unlimited, and equally rich are the physics that underlies the self-assembly of these novel shape amphiphiles and the structures that they could create. Physical structural studies on these model shape amphiphiles are currently ongoing in our group and will be discussed in future publications.

Acknowledgements

This work was supported by NSF (DMR-090689) and the Joint-Hope Education Foundation.

Notes and references

1 R. W. Date and D. W. Bruce, *J. Am. Chem. Soc.*, 2003, **125**, 9012–9013.
2 Z. L. Zhang, M. A. Horsch, M. H. Lamm and S. C. Glotzer, *Nano Lett.*, 2003, **3**, 1341–1346.
3 S. C. Glotzer, *Science*, 2004, **306**, 419–420.
4 S. C. Glotzer, M. A. Horsch, C. R. Iacovella, Z. Zhang, E. R. Chan and X. Zhang, *Curr. Opin. Colloid Interface Sci.*, 2005, **10**, 287–295.
5 M. Voronkov and V. Lavrent'yev, *Top. Curr. Chem.*, 1982, **102**, 199–236.
6 R. H. Baney, M. Itoh, A. Sakakibara and T. Suzuki, *Chem. Rev.*, 1995, **95**, 1409–1430.
7 R. M. Laine, *J. Mater. Chem.*, 2005, **15**, 3725–3744.
8 M. F. Roll, M. Z. Asuncion, J. Kampf and R. M. Laine, *ACS Nano*, 2008, **2**, 320–326.
9 D. Cordes, P. Lickiss and F. Rataboul, *Chem. Rev.*, 2010, **110**, 2081–2254.
10 X.-H. Dong, W.-B. Zhang, Y. Li, M. Huang, S. Zhang, R. P. Quirk and S. Z. D. Cheng, *Polym. Chem.*, 2012, **3**, 124–134.
11 W.-B. Zhang, Y. Tu, R. Ranjan, R. M. Van Horn, S. Leng, J. Wang, M. J. Polce, C. Wesdemiotis, R. P. Quirk, G. R. Newkome and S. Z. D. Cheng, *Macromolecules*, 2008, **41**, 515–517.
12 X. Yu, W.-B. Zhang, K. Yue, X. Li, H. Liu, Y. Xin, C.-L. Wang, C. Wesdemiotis and S. Z. D. Cheng, *J. Am. Chem. Soc.*, 2012, **134**, 7780–7787.
13 X. Yu, S. Zhong, X. Li, Y. Tu, S. Yang, R. M. Van Horn, C. Ni, D. J. Pochan, R. P. Quirk, C. Wesdemiotis, W.-B. Zhang and S. Z. D. Cheng, *J. Am. Chem. Soc.*, 2010, **132**, 16741–16744.
14 J. He, K. Yue, Y. Liu, X. Yu, P. Ni, K. A. Cavicchi, R. P. Quirk, E.-Q. Chen, S. Z. D. Cheng and W.-B. Zhang, *Polym. Chem.*, 2012, **3**, 2112–2120.
15 K. Yue, C. Liu, K. Guo, X. Yu, M. Huang, Y. Li, C. Wesdemiotis, S. Z. D. Cheng and W.-B. Zhang, *Macromolecules*, 2012, **45**, 8126–8134.
16 W.-B. Zhang, Y. Li, X. Li, X. Dong, X. Yu, C.-L. Wang, C. Wesdemiotis, R. P. Quirk and S. Z. D. Cheng, *Macromolecules*, 2011, **44**, 2589–2596.
17 Y. Yu and A. Eisenberg, *J. Am. Chem. Soc.*, 1997, **119**, 8383–8384.
18 Y. Yu, L. Zhang and A. Eisenberg, *Macromolecules*, 1998, **31**, 1144–1154.
19 K. Holmberg, B. Jönsson, B. Kronberg and B. Lindman, *Surfactants and Polymers in Aqueous Solution*, Wiley, Chichester, UK, 2nd edn, 2003.
20 W.-B. Zhang, B. Sun, H. Li, X. Ren, J. Janoski, S. Sahoo, D. E. Dabney, C. Wesdemiotis, R. P. Quirk and S. Z. D. Cheng, *Macromolecules*, 2009, **42**, 7258–7262.
21 Y. Li, X.-H. Dong, K. Guo, Z. Wang, Z. Chen, C. Wesdemiotis, R. P. Quirk, W.-B. Zhang and S. Z. D. Cheng, *ACS Macro Lett.*, 2012, **1**, 834–839.
22 I. Ash and M. Ash, *Encyclopedia of Surfactants*, Chemical Pub. Co.: 1980.
23 D. Attwood and A. T. Florence, *Surfactant Systems: Their Chemistry, Pharmacy and Biology*, Chapman and Hall, London, 1983.
24 R. Zana, Mixed Micelles with Bolaform Surfactants, in *Mixed Surfactant Systems*, American Chemical Society, 1992, vol. 501, pp. 292–300.
25 R. Zana, *Curr. Opin. Colloid Interface Sci.*, 1996, **1**, 566–571.
26 X. Zhang and C. Wang, *Chem. Soc. Rev.*, 2011, **40**, 94–101.
27 H. C. Kolb, M. G. Finn and K. B. Sharpless, *Angew. Chem., Int. Ed.*, 2001, **40**, 2004–2021.
28 C. Barner-Kowollik, F. E. Du Prez, P. Espeel, C. J. Hawker, T. Junkers, H. Schlaad and W. Van Camp, *Angew. Chem., Int. Ed.*, 2011, **50**, 60–62.
29 R. K. Iha, K. L. Wooley, A. M. Nyström, D. J. Burke, M. J. Kade and C. J. Hawker, *Chem. Rev.*, 2009, **109**, 5620–5686.
30 A. B. Lowe, *Polym. Chem.*, 2010, **1**, 17–36.
31 C. E. Hoyle and C. N. Bowman, *Angew. Chem., Int. Ed.*, 2010, **49**, 1540–1573.
32 Y. Lv, Z. Lin and F. Svec, *Analyst*, 2012, **137**, 4114–4118.
33 B. S. Sumerlin and A. P. Vogt, *Macromolecules*, 2009, **43**, 1–13.
34 F. J. Feher, K. D. Wyndham, R. K. Baldwin, D. Soulivong, J. D. Lichtenhan and J. W. Ziller, *Chem. Commun.*, 1999, 1289–1290.

35 S. Karanam, H. Goossens, B. Klumperman and P. Lemstra, *Macromolecules*, 2003, **36**, 3051–3060.
36 S. Ates, Y. Y. Durmaz, L. Torun and Y. Yagci, *J. Macromol. Sci., Pure Appl. Chem.*, 2010, **47**, 809–815.
37 K. Gunes, A. I. Isayev, X. P. Li and C. Wesdemiotis, *Polymer*, 2010, **51**, 1071–1081.
38 J. Zhu, Y. Liao and W. Jiang, *Langmuir*, 2004, **20**, 3809–3812.
39 W. Zhang and A. H. E. Müller, *Macromolecules*, 2010, **43**, 3148–3152.
40 B.-S. Kim and P. T. Mather, *Macromolecules*, 2006, **39**, 9253–9260.
41 Y. Li, W.-B. Zhang, I. F. Hsieh, G. Zhang, Y. Cao, X. Li, C. Wesdemiotis, B. Lotz, H. Xiong and S. Z. D. Cheng, *J. Am. Chem. Soc.*, 2011, **133**, 10712–10715.
42 F. M. Menger and J. S. Keiper, *Angew. Chem., Int. Ed.*, 2000, **39**, 1906–1920.
43 F. M. Menger and C. A. Littau, *J. Am. Chem. Soc.*, 1993, **115**, 10083–10090.
44 S. Karaborni, K. Esselink, P. A. J. Hilbers, B. Smit, J. Karthäuser, N. M. Van Os and R. Zana, *Science*, 1994, **266**, 254–256.
45 R. Zana, *Langmuir*, 1996, **12**, 1208–1211.
46 S. Manne, T. E. Schäffet, Q. Huo, P. K. Hansma, D. E. Morse, G. D. Stucky and I. A. Aksayt, *Langmuir*, 1997, **13**, 6382–6387.
47 R. Zana, *J. Colloid Interface Sci.*, 2002, **248**, 203–220.
48 F. M. Menger and B. N. A. Mbadugha, *J. Am. Chem. Soc.*, 2001, **123**, 875–885.
49 W. Hayes, H. M. I. Osborn, S. D. Osborne, R. A. Rastall and B. Romagnoli, *Tetrahedron*, 2003, **59**, 7983–7996.